euspen's 25th International Conference & Exhibition, Zaragoza, ES, June 2025
www.euspen.eu

Indirect tool wear measurement based on spindle power in finishing operations

Xanti Egaña[1], Amrozia Shaheen[2,3*], Pedro J. Arrazola[1] , Giuliano Bissacco[2]

[1] *Faculty of Engineering, Mondragon Unibertsitatea, Loramendi 4, 20500 Arrasate-Mondragón, Spain*
[2] *Technical University of Denmark, Department of Mechanical Engineering, 2800 Kgs. Lyngby,Denmark*
[3] *LEGO System A/S, Aastvej 1, 7190, Billund, Denmark*

* amrsh@dtu.dk

Abstract

Monitoring tool wear is essential for advanced manufacturing systems and intelligent production. The ability to assess tool condition in real time plays a key role in minimizing costs, improving product quality, reducing machine downtimes, and optimizing manufacturing processes. However, accurate tool monitoring in real time remains a significant challenge in industrial applications due to low efficiency of signal processing methods and poor model generalization for machining processes. While tool condition monitoring techniques have been extensively developed for high chip load operations such as roughing, their effectiveness in fine finishing operations remains a challenge. Lower cutting forces and subtler tool wear make traditional monitoring approaches less reliable. In this work, a power-based monitoring system is designed for fine finishing milling operations. Side milling tests are conducted under cutting conditions of low engagement, while indirect monitoring of the cutting process is performed through power signal acquisition. The acquired signal undergoes necessary pre-processing, followed by the extraction of key features related to the tool's wear state. The evolution of these extracted features is analysed and compared with direct tool wear measurements obtained through an on-machine camera-based system. A comparative approach is established to investigate the correlation between spindle power variations and tool wear in fine finishing operations.

Tool condition monitoring, Milling, Tool wear, Finishing.

1. Introduction

Conventional machining operations, such as turning, milling, grinding, and drilling, are indispensable in the modern manufacturing industry. Monitoring the state of cutting tools used in machining processes is essential, as 3-12% of the production cost is closely related to the condition of cutting tools and their replacement. Cutting tool wear not only increases production costs but also contributes to machine downtime, cutting tool failures (wear and breakage) typically represent around 20% of a machine tool's downtime [1]. Furthermore, an accurate and reliable tool condition monitoring (TCM) system could result in cutting speed increases of 10–50% [2].

Real-time tool wear monitoring, thus performed during the cutting process, can only be achieved through indirect means, by inferring the wear condition from signals correlated to the wear process. Furthermore, an industrially viable tool wear condition solution must be non-invasive, to maximize efficiency and maintain productivity. Indirect monitoring for high-chip load operations is well established, but monitoring for finishing operations is challenging due to the small acceptable wear levels and the related small variation of the load. Some of the quantities measurable in-process representing the tool condition are acoustic emissions (AE) [3], cutting forces [4], vibration signals [5], spindle torque, spindle power [6], and thermal imaging [7].

Some studies show that power sensors could replace the cutting force sensors (which are usually invasive) for industrial tool wear monitoring [8]. In power-based monitoring, the load-related spindle power in finishing operations is a small fraction of the power used [9], and wear creates small variations in the load-related fraction. In addition, signal to noise ratio in finishing operations is very low. Apart from that, milling operations are considerably more difficult to monitor than operations with continuous engagement, because of the multiple teeth of the cutting tool and variable chip thickness.

In this paper spindle power based TCM in fine finishing operations has been demonstrated by implementing high resolution spindle power monitoring and signal preprocessing techniques. Relevant features are extracted from the signal, and the effectiveness of the method is validated through comparison with direct wear measurements.

2. Experimental setup

Figure 1 shows the schematic of the experimental setup for indirect tool wear monitoring. The workpiece is mounted on a vice on top of a dynamometer on a machine tool (FANUC ROBODRILL α-D21LiB5adv). The data acquisition for power signal is acquired using a current sensor (Montronix PS200-NG) which transmits an analogue output signal to the acquisition devices (NI DAQ) where the signal is discretized. The machine tool sends a 24 V signal (a pulse of 24 V and 1 s duration) to the DAQ. The trigger signal of 24V goes through the voltage divider and initiates the data acquisition process. The acquired signal is converted into power by multiplying with the scaling factor.

The camera-based system (CBS) is an optical system mounted on the machine tool. The CBS is used as a tool presetting system for measuring the cutting tool geometry in machining operations. The optical system comprises of a camera and an illumination unit and captures the images of the rotating milling tool at different rotating angles. This information is later post-processed for radial wear estimation by comparing against the

reference model of a new clean tool. Figure 2 shows an image of the CBS. Force data acquisition was performed simultaneously with power data acquisition but not included in this work.

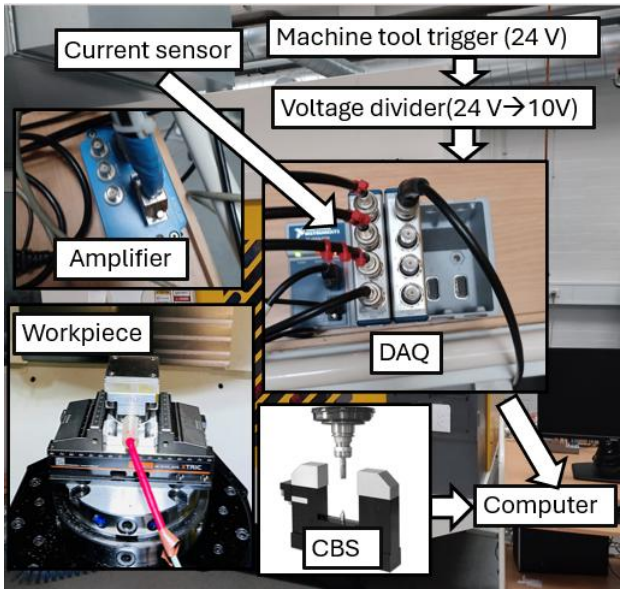

Figure 1 Experimental setup with the workpiece mounted on a dynamometer and accessories (signal amplifier, data acquisition system (DAQ)).

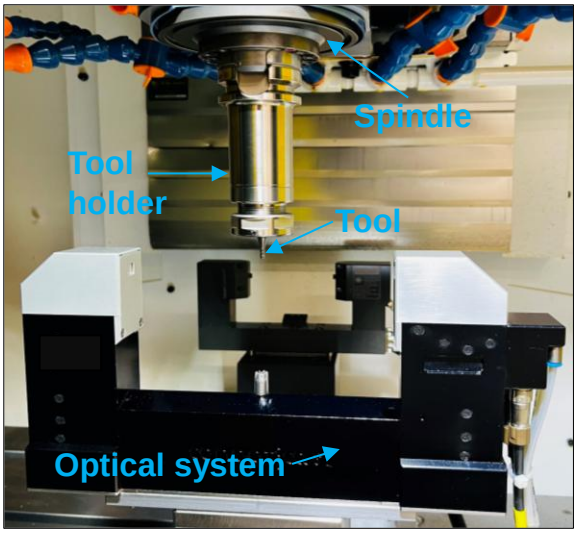

Figure 2 A photograph of the camera-based system with Ø3 mm radius end mill mounted in the spindle of the machine tool.

The cutting tool used is Ø3 mm radius end mill (MHDH445R by NS Tool) with a helix angle of 45˚. It has four flutes and a nose radius of 0.2 mm. The rake angle on the cylindrical part of the cutting tool is -20˚. Figure 3 shows the cutting tool-workpiece engagement in the side milling operation. The workpiece material was a chromium-molybdenum-vanadium hardened steel (AISI H13 hot-work steel, classified according to NADCA #207 Grade B) with hardness of 48-50 HRC. Dedicated workpieces with grooves of 1 mm depth were prepared to restrict the tool engagement on the cylindrical part of the tool.

Side milling tests have been performed under cutting conditions of low engagement similar to fine finishing operations and by engaging the 1 mm region on the cylindrical region of the cutting tool. The milling process parameters are listed in Table 1. The milling parameters were kept constant for all four cutting tools used in the tests.

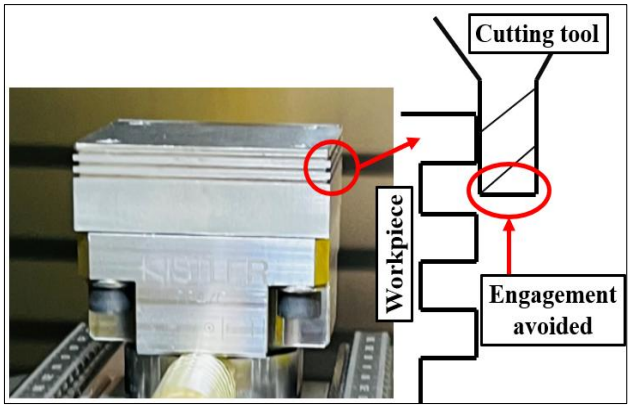

Figure 3 Tool-workpiece engagement.

Table 1. Cutting conditions for the side milling operation.

Cutting conditions	
Spindle speed	6366 RPM
Axial depth of cut	1 mm
Radial depth of cut	0.05 mm
Cutting speed	60 m/min
Table feed per minute	480 mm/min
Feed per tooth	0.019 mm/tooth
Sampling rate (for acquisition)	100 kHz

3. Data processing

The data related to power is processed and the most important features are extracted. The power signal in the engaged zone is normalized with respect to the power signal in the non-engaged zone. Figure 4 shows the zone in which the tool is engaged (orange curve) and the zone in which the tool is not engaged (blue curve).

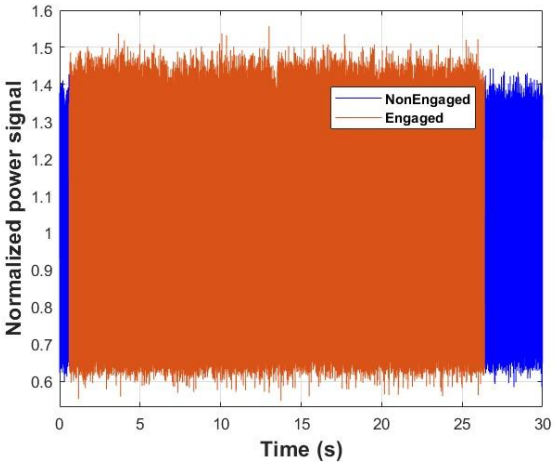

Figure 4 Power versus time graph showing the engaged and non-engaged zones of the power signal.

Two features are extracted from the power signal; the mean power signal and the amplitude of the wave of the signal [10]. The baseline of the power signal varies with time due to various factors such as spindle temperature, and spindle lubrication. In order to test the validity of the feature extraction method, the analysis of the selected features is performed by comparing them with the same feature from the baseline power signal. The features are calculated for the engaged zone and the non-

engaged zone, and then the features of the engaged zone are normalized with respect to the non-engaged zone to obtain the signal feature that is used as a measurement parameter. The representation of the normalized moving average of the power with respect to the power signal is shown in Figure 5, showing the 4 machined zones (4 straight segments of tool path).

As for the power amplitude, an algorithm is implemented to detect the maximum and minimum peaks of the power signal, and these peaks are used to calculate the average amplitude, and depicted in Figure 6.

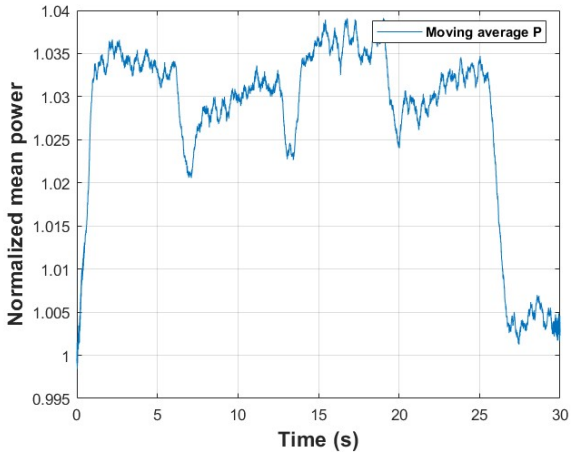

Figure 5 Power versus time graph showing the moving average of the power signal.

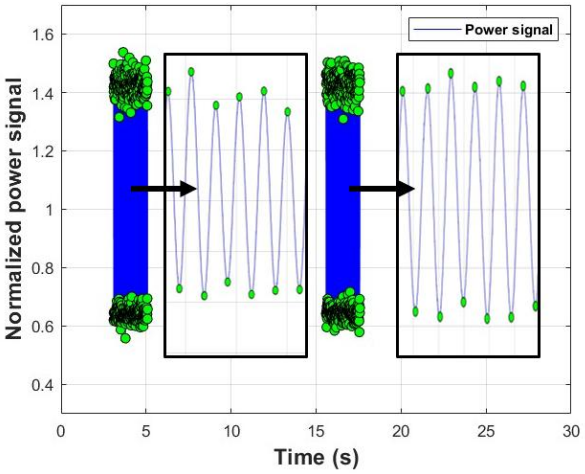

Figure 6 Power versus time graph showing peak selection (green circles) on the acquired data and the zoomed-in view. The two datasets with selected peaks correspond to the two segments of the acquired signal.

4. Results

4.1. Results for extracted features

The progression of the extracted features (normalized mean power and the normalized power amplitude) with respect to the cutting length for four cutting tools is analysed. Figure 7 shows the evolution of the normalized mean power with the cutting length for the four tools being tested. The normalized mean power shows a general upward trend, although some data points show dispersion.

The progression of the normalized power amplitude feature with cutting length is shown in Figure 8. In this case, the trend of the extracted feature is ascending and depicting a relatively lower dispersion as compared to the other extracted feature from power data (see Figure 7).

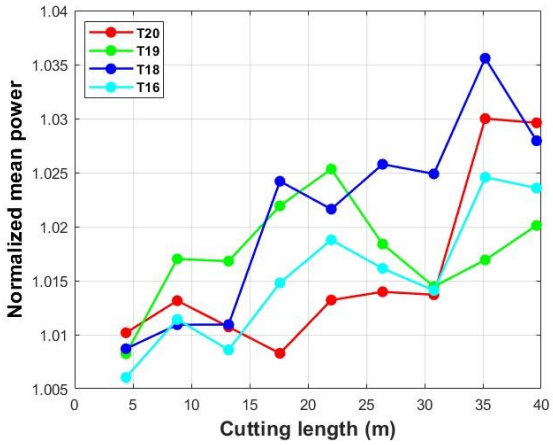

Figure 7 Normalized mean power evolution vs cutting length.

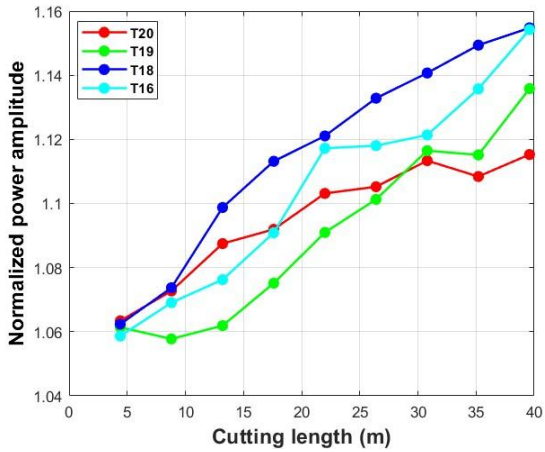

Figure 8 Normalized power amplitude evolution vs cutting length.

4.2. Comparison with direct measurement

The results obtained with indirect monitoring are compared with the average radial wear values obtained with CBS. The average radial wear for the CBS is computed by taking an average on the difference of the new and the worn tool profiles in the engaged 1 mm zone. Results obtained for one of the tools (labelled as T16) are shown in Figure 9. A clear correlation is seen between power amplitude and average radial wear. As can be seen, high resolution power measurement enables wear monitoring even for very low radial wear values of only few µm.

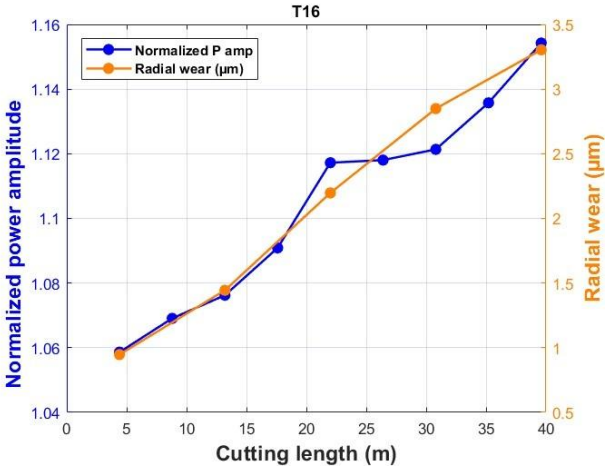

Figure 9 Relation between normalized power amplitude and radial wear for T16.

Figure 10 shows the normalized power amplitude for all tools against their respective average radial wear. Considering that the wear behaviour is roughly linear over the explored range (steady state wear rate), a linear fit with all the data points is used. The black line represents the general trend, and the dotted black lines are plotted with a 95% confidence interval.

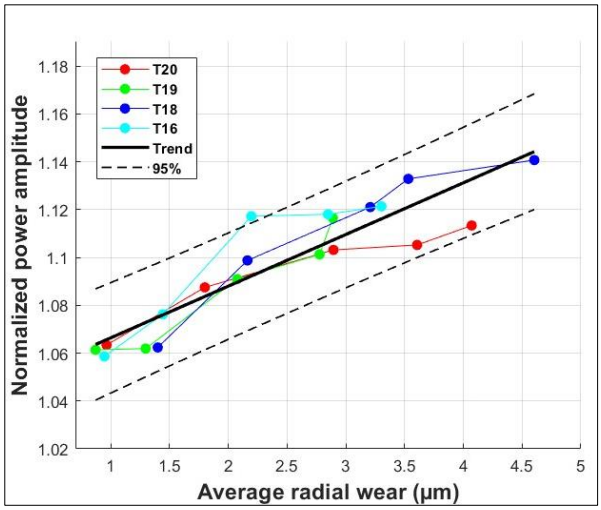

Figure 10 Relation between normalized power amplitude and average radial wear.

4.3. Discussion

The combination of a high resolution power measurement device and data processing algorithms has shown the ability to correctly reveal the wear trend of small cutting tools in a light machining operation characterized by a small uncut chip thickness and chip cross section, representative of finishing machining operations. The system was tested for cutting lengths generating very small amounts of wear, with maximum observed radial wear of 4.5 µm. A clear relationship is seen between the extracted features and radial tool wear as measured by the CBS in the very low wear range, demonstrating the suitable sensitivity of the system. Figure 10 indicates that all the data points obtained follow a similar trend and they all reside within an approximate range of 4% of the normalized value of the power amplitude feature.

5. Conclusions

In this work, we have developed an indirect tool wear monitoring system for milling finishing operations based on spindle power. The highly sensitive system can detect small changes in wear values using power related features. However, the definition of the extracted features can be optimised to increase the precision of the monitoring system.

Future work will focus on identifying signal features yielding improved results in terms of robustness towards the estimation of radial wear. Frequency domain analysis techniques, machine learning algorithms, or deep learning methods will be explored to extract additional information from the signals obtained during machining. The robustness of the approach will be further validated in various engagement conditions.

References

[1] Chen Zhang and Jilin Zhang 2013 *ScienceDirect* **64** 708
[2] Adam G. Rehorn, Jin Jiang and Peter E. Orban 2005 State of the art methods and results in tool condition monitoring: a review *Springer Nature* **26** 693
[3] Didem Ozevin 2020 MEMS Acoustic Emission Sensors *mdpi* **10** 8966
[4] Mustafa Kuntoğlu, Abdullah Aslan, Danil Yurievich Pimenov, Üsame Ali Usca, Emin Salur, Munish Kumar Gupta, Tadeusz Mikolajczyk, Khaled Giasin, Wojciech Kapłonek and Shubham Sharma 2021 A Review of Indirect Tool Condition Monitoring Systems and Decision-Making Methods in Turning: Critical Analysis and Trends *mdpi* **21** 108
[5] Ayman Mohamed, Mahmoud Hassan, Rachid M'Saoubi and Helmi Attia 2022 Tool Condition Monitoring for High-Performance Machining Systems—A Review *mdpi* **22** 2206
[6] R. Teti, D. Mourtzis, D.M. D'Addona and A. Caggiano 2022 Process monitoring of machining *ScienceDirect* **71** 529
[7] T. Mohanraj, S. Shankar, R. Rajasekar, N.R. Sakthivel and A. Pramanik 2020 Tool condition monitoring techniques in milling process - a review *ScienceDirect* **9** 1032
[8] Qun Wang, Hengsheng Wang, Liwei Hou and Shouhua Yi 2021 Overview of Tool Wear Monitoring Methods Based on Convolutional Neural Network *mdpi* **11** 12041
[9] Nitin Ambhorea, Dinesh Kambleb, Satish Chinchanikara and Vishal Wayala 2015 Tool condition monitoring system: A review *ScienceDirect* **2** 3419
[10] Xiang Wang, Yuan Zheng, Zhenzhou Zhao and Jinping Wang 2015 Bearing Fault Diagnosis Based on Statistical Locally Linear Embedding *mdpi* **15** 16225